

## PERIODIC ORBITS IN TRIANGULAR BILLIARDS\*

TH.W. RUIJGROK

Institute for Theoretical Physics  
Princetonplein 5, P.O.Box 80006, 3508 TA Utrecht, The Netherlands

(Received July 9, 1991)

From all orbits described by a ball bouncing elastically inside a triangular billiard some special classes are selected for further numerical investigation. One of these classes consists of all orbits starting in a direction perpendicular to a side. Evidence is presented to show that almost all orbits of this kind are either periodic or end in a corner. The starting points with the same period form intervals, which are distributed in some regular fashion. Even for orbits with very high period the phase portrait and the velocity portrait show peculiar regularities. Although these observations suggest a number of theorems with general validity, the author cannot support them with more than plausibility arguments.

PACS numbers: 05.45.+b

## 1. Introduction

The triangular billiard is one of the simplest dynamical systems and yet its qualitative features are not fully understood.

An excuse to study this billiard is found in the fact that for rectangular triangles it is equivalent to two hard balls moving on a line and colliding with the walls and with each other [1-5]. For such a system it is natural to ask questions about its behaviour during very long times. Typical questions are:

1. is there a dense orbit in phase space, i.e., is the system *topological transitive*?
2. does every orbit lie dense in phase space, i.e., is it *minimal*?
3. is the measure of every invariant set in phase space either zero or unity, i.e., is it *ergodic*?

---

\* Presented at the XXXI Cracow School of Theoretical Physics, Zakopane, Poland, June 4 - 14, 1991.

4. are there ergodic subsets, *i.e.*, are there *ergodic components*?
5. is for all  $f$  and  $g$   $\lim_{t \rightarrow \infty} \int f(T_t x)g(x)d\mu = \int f(x)d\mu \cdot \int g(x)d\mu$ , *i.e.*, is it *mixing*?
6. is the distance between two points in phase space growing exponentially in time, *i.e.*, is it a *K-system*?
7. are there *periodic orbits*?
8. are there *aperiodic orbits* and if so are they dense in all of phase space (*aperiodic dense*) or in a subset (*aperiodic local*)?

It is expected that, if these questions can be answered for polygonal billiards, the insight gained will also apply to more realistic systems.

The following is a short list<sup>1</sup> of the main result for these billiards. A review, giving the state of the art in 1986, was written by Gutkin [6].

1973: Sinaï [3] proves the non-ergodicity of rational billiards.

1976: In a numerical study Casati and Ford [2] show that triangles with irrational ratio's of the angles probably are mixing.

1976: For almost all starting directions the flow on a rational billiard is minimal (Zemlyakov and Kato [7]).

1978: Boldrighini, Keane and Marchetti [8] prove that for almost all starting directions every orbit comes arbitrarily close to at least one vertex. Using this theorem, they then show that the entropy is zero.

1980: Katok [9] proves that rational billiards are not mixing.

1983: There is a triangle with an aperiodic local orbit [5].

1986: According to Masur [10] every rational billiard has a dense set of directions each with a periodic orbit.

Open questions are among others whether every irrational triangle (i) is ergodic, (ii) has an aperiodic local orbit and (iii) has a periodic orbit. In this paper the first two questions will be left untouched. The problem of periodic orbits, however, will be investigated in some detail, mainly by applying numerical methods.

An orbit is described by giving the series of triples  $(i_0, f_0, \theta_0)$ ,  $(i_1, f_1, \theta_1)$ ,  $\dots$ ,  $(i_k, f_k, \theta_k)$ ,  $\dots$ , where  $i$  is the side which was just hit by the bouncing ball,  $f$  is the collision point on that side, with the side length as unit and  $\theta$  is the angle between orbit and side. See figure 1. The relation between the angles for a collision  $(\theta, i) \rightarrow (\theta', j)$  is given by

$$\theta' = \pi - \theta - \sum_{k=1}^3 \epsilon_{ijk} \alpha_k, \quad (1.1)$$

---

<sup>1</sup> With thanks to T.H.M. Dijkstra for its compilation.

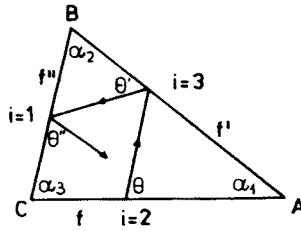


Fig. 1. Definition of  $f, \theta$  and side number  $i$

where  $\epsilon_{ijk}$  is the completely antisymmetric tensor and the angles of the triangle are denoted by  $\alpha_1, \alpha_2$  and  $\alpha_3$ .

Equation (1.1), because of its simplicity, suggests to define two classes of special orbits, namely:

1. *Integer orbits*, for which each collision angle  $\theta$  can be written as  $\theta = q_1\alpha_1 + q_2\alpha_2 + q_3\alpha_3$  with integer  $q_\ell$ . From Eq. (1.1) it then follows that the next angle is also of this form,  $\theta' = q'_1\alpha_1 + q'_2\alpha_2 + q'_3\alpha_3$ , with

$$q'_k = 1 - q_k - \epsilon_{ijk} \quad \text{if } i \text{ and } j \text{ are successive sides.} \quad (1.2)$$

2. *Half-integer or orthogonal orbits*, for which each collision angle  $\theta$  can be written as  $\theta = q_1\alpha_1 + q_2\alpha_2 + q_3\alpha_3 + \pi/2$ , again with integer  $q_\ell$ . The next angle is then again of this form,  $\theta' = q'_1\alpha_1 + q'_2\alpha_2 + q'_3\alpha_3 + \pi/2$ , with

$$q'_k = -q_k - \epsilon_{ijk} \quad \text{if } i \text{ and } j \text{ are successive sides.} \quad (1.3)$$

If at one and only one point a half-integer orbit hits a side perpendicularly, which for an irrational triangle is only possible if  $q_1 = q_2 = q_3 = 0$ , the orbit will be called *mono-orthogonal*. If there is a second point on such an orbit where this happens, the orbit will be called *bi-orthogonal*. A bi-orthogonal orbit of course is periodic. The orbit is called *weak-orthogonal* if for all points  $\theta \neq \pi/2$ . Many years ago [4] it was discovered that for every irrational rectangular triangle almost every orbit, which starts perpendicularly from the hypotenuse is most probably periodic and therefore bi-orthogonal with the above definition.

The present paper is a report about a more extensive search for periodic orbits in the classes of integer- and half-integer orbits. The results can be expressed in the form of four conjectures, supposedly valid for any irrational triangle:

*1st Conjecture:* Almost all mono-orthogonal orbits are bi-orthogonal and therefore periodic.

*2nd Conjecture:* When considering all integer periodic orbits which start with a given angle from a certain side, then all these starting points form a set of intervals which cover that side densely.

*3rd Conjecture:* The set of weak-orthogonal periodic orbits is empty.

*4th Conjecture:* In an irrational triangle a periodic orbit is either integer or bi-orthogonal.

The first conjecture can be made plausible using a statistical argument. Let  $s = \pm 1$  indicate whether the number of collisions since the start of the orbit is even or odd. Then after one step  $s' = -s$ . If  $r_k = sq_k$ , it follows from Eq. (1.3) that  $r'_k = r_k + s\epsilon_{ijk}$ . In each step, therefore, only one component of the vector  $\vec{r} = (r_1, r_2, r_3)$  is changed by  $+1$  or  $-1$ . Since the orbit is assumed to be mono-orthogonal, the starting point can be taken at the origin  $\vec{r} = (0, 0, 0)$  of the 3-dimensional cubic lattice. The collision sequence generates a walk on this lattice, but since  $0 < \theta < \pi$  the walk is such that  $-\pi/2 < \vec{r} \cdot \vec{\alpha} < \pi/2$ , where  $\vec{\alpha} = (\alpha_1, \alpha_2, \alpha_3)$ . If the actual path is replaced by a random walk, this condition is no longer automatically satisfied, but must be imposed. The path, therefore, is effectively a random walk on a 2-dimensional lattice. For this case the random walker will return to the origin with one hundred percent probability. This recurrence means that the orbit again hits a side under ninety degrees, which implies the first conjecture. For rectangular triangles additional (and better) evidence will be presented in the next Section, while arbitrary triangles are considered in Section 3.

The other conjectures have a lower status and are mainly based on examples to be given in Sections 4 and 5.

The pictures which will be shown in the following Sections are mainly of two types. In the first, of which two examples are given in Fig. 2, the circumference of the triangle, i.e., BCAB, is put on the horizontal axis with the length of each side normalized to unity. The vertical axis is for the reflection angle ranging from 0 to 180 degrees. Every point in this "phase portrait" now fully represents the collision with a side.

The second type of picture, the "velocity portrait", shows the way in which, during a collision sequence, the velocity vector of the billiard ball has been changing. In each collision with a side  $i$ , the new velocity vector is obtained by reflecting the previous one in a line through the origin which is parallel to side  $i$  of the triangle. Two successive reflections, first  $T_k$  and then  $T_j$ , amount to a rotation around an axis perpendicular to the plane. More specifically  $D_i = T_j T_k$  is an anti-clockwise rotation over  $2\alpha_i$ , where  $(ijk)$  is a cyclic permutation of  $(123)$ . The three rotations  $D_1, D_2$  and  $D_3$  commute among each other,  $D_i^{-1} = T_k T_j$  and  $D_1 D_2 D_3 = 1$ . In a series of  $2n$  collisions the velocity vector therefore suffers  $n$  rotations, each over one of the six angles  $\pm 2\alpha_1, \pm 2\alpha_2, \pm 2\alpha_3$ . If one such rotation is represented by a

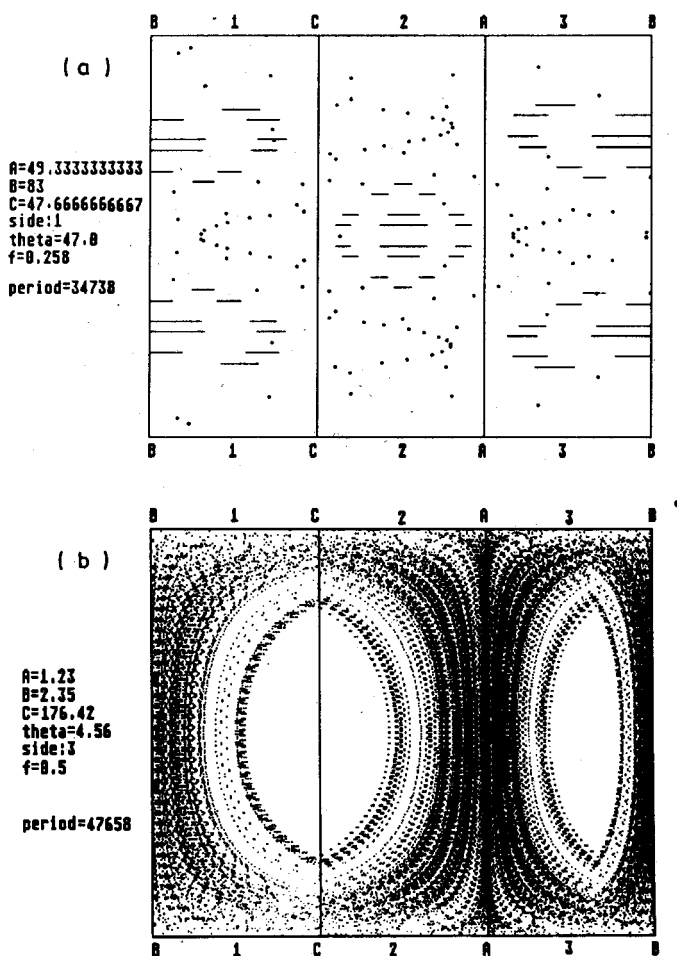


Fig. 2. Examples of phase portraits. (a)  $A = 49.33333333$ ,  $B = 83.0$ ,  $C = 47.66666667$ ,  $\theta = 47.0$ ,  $i = 1$ ,  $f = 0.258$ ,  $\text{period} = 34738$ . (b)  $A = 1.23$ ,  $B = 2.35$ ,  $C = 176.42$ ,  $\theta = 4.56$ ,  $i = 3$ ,  $f = 0.5$ ,  $\text{period} = 47658$ .

unit vector of a hexagon (see Fig. 3), the rotation after a number of collisions can be written as  $D_1^k D_2^\ell$ , where  $k$  and  $\ell$  are uniquely determined. In the velocity portrait this rotation is represented by a point with coordinates  $(k, \ell)$  along the  $D_1$ - and  $D_2$ -axis.

For a periodic orbit in an irrational triangle it is necessary, but not sufficient, that the values of  $k$  and  $\ell$  of the endpoint of the orbit are equal to  $k = \ell = 0$ . For a rectangular triangle with  $\alpha_2 = \pi/2$ , the orbit can also be periodic if  $k = 0$  and  $\ell$  even. Two examples of the resulting picture are

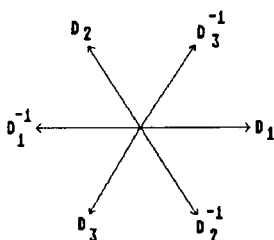


Fig. 3. Representation of rotations of velocity vectors after two collisions

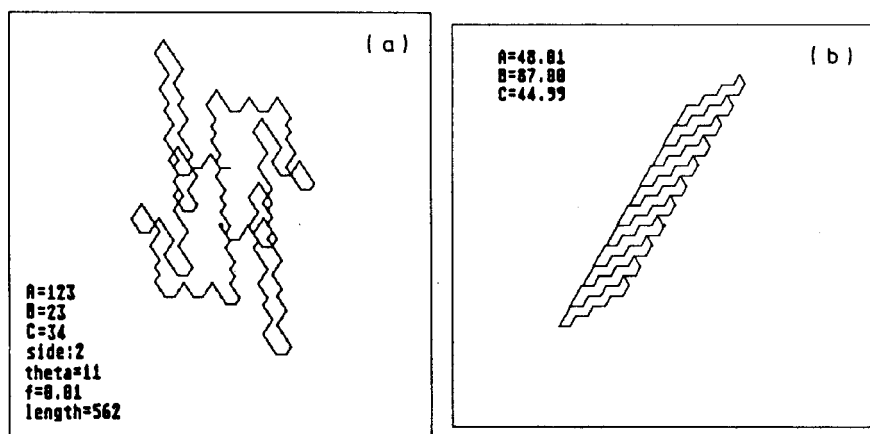


Fig. 4. Two examples of velocity portraits

given in Fig. 4. This example also shows that the motion does not very much resemble that of a random walker. Therefore, if periodic orbits will be found, it will be necessary to explain their existence on other grounds than with statistical arguments.

## 2. Bi-orthogonal orbits in a rectangular triangle

By looking at Fig. 5 the reader can easily convince himself that any rectangular triangle has a bi-orthogonal orbit with period 6. Actually, assuming that  $\alpha < \pi/4$ , every point of the hypotenuse at a distance less than  $c$  from the corner  $C$  is the beginning and the end of such a period-6 bi-orthogonal orbit. When the starting point, denoted by a black square, is moved into the direction of the arrow, the other collision points also move as indicated. The endpoint  $c$  of the period-6 interval is reached when two of these points coalesce in a corner. The figure shows that  $c$  is the orthogonal endpoint of a ball which is launched at  $C$  with an elevation  $\pi/2 - 2\alpha$ . From this follows

that, when the hypotenuse has unit length, the value of  $c$  is  $2\sin^2 \alpha$ . The point  $b$  is defined as the location where the hypotenuse is hit perpendicularly by an orbit, which started from  $B$  into a direction  $\alpha$  with respect to the side  $BC$ . This point divides the periodic interval into two equal parts. This property holds for all periodic intervals and is a consequence of the "reflector theorem", which is shown and proved in Fig. 6.

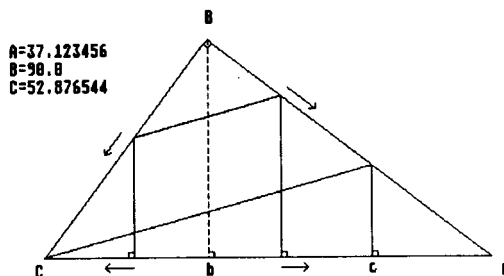


Fig. 5. Bi-orthogonal orbits for a rectangular triangle

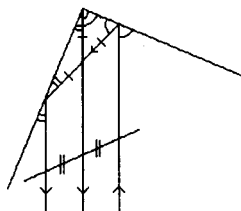


Fig. 6. The "reflector theorem"

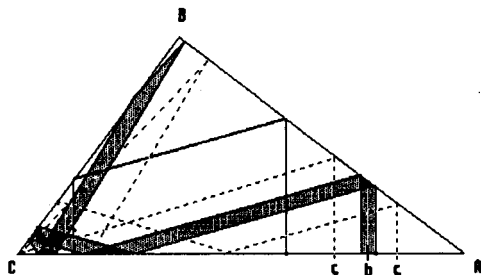


Fig. 7. Construction of a period-22 orbit

If the starting point on the hypotenuse is moved to the right of  $c$ , a new interval of period-22 points appears. This is seen in Fig. 7. Because

of the reflector theorem the left side and the right side of the bundle are always parallel, which proves the periodicity. Determining the period itself is a matter of counting. Before this can be done, however, the order must be established in which the sides are touched by the orbit. Especially when the orbit comes close to a corner this requires an accurate numerical calculation. This also shows that the period will depend on  $\alpha$ . The upper limit on the base line of the period-22 interval is again reached by an orbit leaving  $C$  with an angle commensurate with  $\alpha$  and  $\pi/2$ , i.e., of the form  $(p+1)\pi/2 + q\alpha$ , where  $p$  and  $q$  are integer numbers. In this case  $p = 2$  and  $q = -6$ . The lower limit was obtained with  $p = 0$  and  $q = -2$ . The  $b$ -point in the middle of this interval is reached by an orbit starting from  $B$  also with a commensurate angle of the form  $(p+1)\pi/2 + q\alpha$ , but with  $p = -3$  and  $q = 5$ . The reason why the upper limit of the periodic interval is indeed reached by an orbit leaving  $C$  (and not  $A$  or  $B$ ) is seen in Fig. 8. When the point "in" is moved in the direction of  $C$  also the point "out" moves in the same direction. The number of infinitesimal orbit elements necessary to turn an incoming ball into an outgoing one is denoted by  $\epsilon$ . In the example of Fig. 8 its value is  $\epsilon = 3$ . For an angle of ninety degrees or larger  $\epsilon = 1$ , while for acute angles  $\epsilon$  is at most equal to the number of times the angle is contained in  $\pi$ .

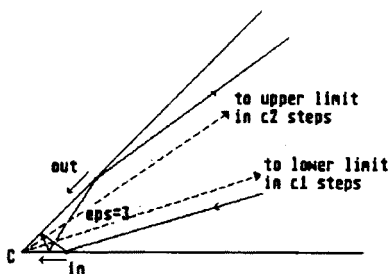


Fig. 8. Turning through a corner

From the construction in Fig. 7 it is seen that, if  $c_1$  is equal to the number of path elements of the orbit from  $C$  to the lower limit of the periodic interval, and  $c_2$  the corresponding number of the other orbit to the upper limit, then half the period is equal to  $\frac{1}{2}P = c_1 + c_2 + \epsilon$ .

The same half period can also be calculated from the number of path elements of the orbit from  $B$  which follows the centre of the bundle and hits the base line perpendicularly in the middle of the periodic interval. If this number is  $b$  then  $\frac{1}{2}P = 2b + 1$ .

These two relations can also be written as

$$P = 2(2b + 1) \quad (2.1)$$

and

$$\epsilon = 2b + 1 - c_1 - c_2. \quad (2.2)$$



For the orbit shown in Fig. 7 these variables have the following values:  $b = 5$ ,  $c_1 = 2$ ,  $c_2 = 6$  and  $\epsilon = 3$ .

The process of moving the starting point to the right can be repeated over and over again, where each time a new periodic interval is found, with lower and upper limits which can be reached from  $C$  by following orbits with starting angles of the form  $(p + 1)\pi/2 + q\alpha$ . The midpoint of such an interval is reached from  $B$  with a starting angle of the same form.

In this way an infinite series of periodic  $cbc$ -intervals is constructed, with an accumulation point, which, however, is not the endpoint  $A$ . By starting from  $A$  a similar set of periodic intervals can be constructed, of which the midpoint is again reached from  $B$ , but the lower and upper limits are now  $a$ -points. An example of a bi-orthogonal orbit of this type is shown in Fig. 9.

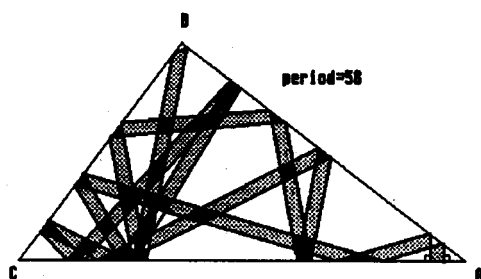


Fig. 9. Family of period-58 orbits with  $A$  as singular corner

In this way the whole base line is covered with intervals, so that every point of a given interval is the starting point of a bi-orthogonal orbit, with a period which is characteristic for the interval. The same process can be repeated for the other two sides of the rectangular triangle.

The truth of the above statement still depends on the validity of the assumption that at the half way point each orthogonal orbit passes the rectangle  $B$  close enough, so that on its way back it remains parallel to the part of the orbit leading up to  $B$ . In spirit this is similar to the theorem of Boldrighini, Keane and Marchetti, quoted above [8], but not the same. The reader is invited to give the proof, since the author was unable to do so. There is, however, overwhelming numerical evidence for the truth of the first conjecture, which will now be presented.

For a rectangular triangle with  $\alpha = (\sqrt{5} - 1)\pi/6 \simeq 37.082\dots$  a large number of orbits was constructed which began in a corner in a direction  $(p + 1)\pi/2 + q\alpha$  and ended orthogonal to one of the sides. The value of  $q$  was varied between  $-100$  and  $+100$ . For each  $q$  the value of  $p$  is fixed. After each collision  $p$  and  $q$  have again integer values, so that the decision whether the final angle is indeed ninety degrees is simple:  $p$  and  $q$  must

TABLE I

Partitioning of side  $B - C$  of rectangular triangle into intervals with period =  $2(2b + 1)$ .  $a$  = length of orthogonal orbit leaving  $A$ .  $b$  = length of orthogonal orbit leaving  $B$ .  $c$  = length of orthogonal orbit leaving  $C$ .  $(p + 1) * 90 + q * A$  = starting angle.  $x$  = position on  $B - C$ , where orbit hits side perpendicularly.  $\epsilon$  = number of turn around collisions.  $\epsilon = 2b + 1 - a_1 - a_2$  or  $\epsilon = 2b + 1 - c_1 - c_2$ .

<i>ABC</i>	<i>p</i>	<i>q</i>	<i>x</i>	<i>a</i>	<i>b</i>	<i>c</i>	$\epsilon$	period
<i>B</i>	0	-2	0.116511		7		4	30
<i>A</i>	1	-4	0.233023	11				
<i>B</i>	2	-6	0.310234		45		4	182
<i>A</i>	-5	10	0.387445	76				
<i>B</i>	4	-12	0.387524		9343		4	37374
<i>A</i>	5	-14	0.387604	18607				
<i>B</i>	12	-30	0.387607		202435		4	809742
<i>A</i>	?	?	0.387610?	386260?				
<i>B</i>	10	-26	0.387614		226845		4	907382
<i>A</i>	9	-24	0.387618	67427				
<i>B</i>	8	-20	0.387652		68599		4	274398
<i>A</i>	-13	30	0.387687	69768				
.	.	.	.		.		.	.
.	.	.	.		.		.	.
.	.	.	.		.		.	.
.	.	.	.		.		.	.
<i>C</i>	3	-9	0.387691			119795		
<i>B</i>	22	-54	0.387725		61733		2	246934
<i>C</i>	-3	5	0.387760			3670		
<i>B</i>	-4	8	0.388577		1840		3	7362
<i>C</i>	-1	1	0.389395			8		
<i>B</i>	-2	4	0.694697		4		1	18

both be zero. The only question therefore, is whether for each collision, especially for those with a collision point close to a corner, the collision side was identified properly. For the longest orbit found, with a length of more than two million steps, the shortest distance to a corner was  $5.10^{-7}$ , with a hypotenuse of unit length. For all other orbits this distance was larger. Although this is a small number, it is still very large compared to the accuracy with which the endpoint of the orbit could be determined, which is of the order of  $10^{-12}$ . This was verified for the longest orbits by taking an arbitrary starting point from the interval claimed to be periodic,

and letting the ball follow the orthogonal orbit for the full period.

The results are given in the Tables I, II and III for the division of the sides opposite to the corners  $A$ ,  $B$  and  $C$  respectively. The first column gives the corner from which the orbit started:  $p$  and  $q$  determine its direction;  $x$  is where it hits the side perpendicularly;  $a$ ,  $b$  or  $c$  is the number of steps;  $\epsilon$  is the number of turnarounds in a corner; the last column gives the period  $2(2b + 1)$  for each point in the interval. The small values of  $\epsilon$  testify to the fact that there are no gaps between successive intervals, except at the accumulation points, of which there seems to be only one per side.

One orbit from  $B$  to the side opposite  $C$  (Table III) has a question mark. It should have the period 612578 if  $\epsilon = 2$ , but has not really been found.

The phase portrait of a rather long bi-orthogonal orbit is shown in Fig. 10. The most conspicuous feature of this picture is that only a small number of different reflection angles occur. Also curious is the symmetry of the figure: with every  $\theta$  also  $\pi - \theta$  occurs. The explanation is simple: every orbit which is sufficiently long, will consist of many parts running parallel to each other and at close distance, but in opposite direction, because of the reflector property of the ninety degree angle at  $B$ .

The motion, therefore, is certainly not one of a random walker, which in the first Section was suggested as a possible explanation of the periodic orbits. The same can be said about the velocity portrait, Fig. 11, for the same orbit.

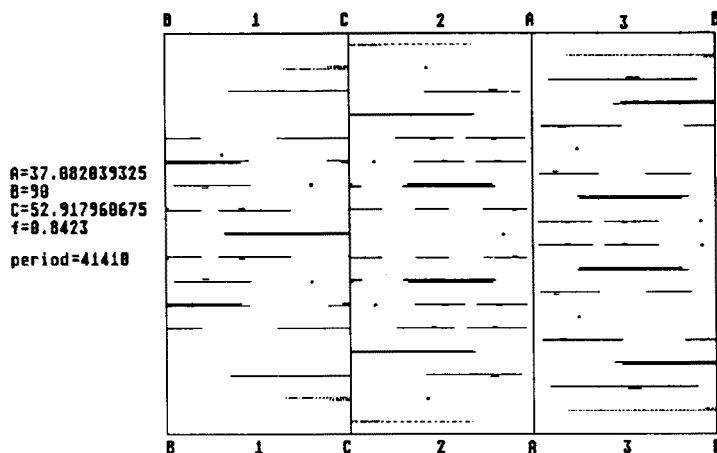


Fig. 10. Phase portrait of bi-orthogonal orbit with period 41410.  $A = 37.082\dots$ ,  $B = 90.0$ ,  $C = 52.91\dots$ ,  $f = 0.8423$ .

TABLE II

Same as Table I for side  $C - A$ 

$ABC$	$p$	$q$	$x$	$a$	$b$	$c$	$\epsilon$	period
$B$	-1	1	0.363558		1		1	6
$C$	0	-2	0.727116			2		
$B$	-3	5	0.783966		5		3	22
$C$	2	-6	0.840816			6		
$B$	5	-13	0.841381		2806		2	11226
$C$	-4	8	0.841947			5605		
$B$	-5	11	0.842120		8345		2	33382
$C$	4	-12	0.842293			11084		
$B$	11	-27	0.842334		10352		3	41410
$C$	6	-16	0.842375			9618		
$B$	-9	21	0.842376		48501		2	194006
$C$	-8	18	0.842377			87383		
$B$	-3	7	0.842397		43741		3	174966
$C$	-10	22	0.842417			97		
$B$	-23	55	0.842437		2445		2	9782
$C$	10	-26	0.842456			4792		
$B$	-19	45	0.842493		9257		2	37030
$C$	-12	28	0.842530			13721		
$B$	-15	35	0.842532		232501		3	930006
$C$	-14	32	0.842534			451279		
$B$	-17	39	0.842538		228237		2	912950
$C$	14	-36	0.842541			5194		
.	.	.	.	.		.	.	.
.	.	.	.	.		.	.	.
.	.	.	.	.		.	.	.
.	.	.	.	.		.	.	.
$A$	16	-41	0.842544	7586				
$B$	-7	15	0.842562		5779		4	23118
$A$	-16	37	0.842579	3969				
$B$	7	-17	0.842584		6854		4	27418
$A$	12	-31	0.842589	9736				
$B$	17	-43	0.842654		6716		4	26866
$A$	-12	27	0.842720	3693				
$B$	7	-19	0.842784		7898		4	31594
$A$	8	-21	0.842848	12100				
$B$	-13	31	0.842850		7419		4	29678
$A$	-8	17	0.842852	2735				
$B$	9	-23	0.844130		1614		3	6458
$A$	-6	13	0.845408	491				

TABLE II continued

<i>ABC</i>	<i>p</i>	<i>q</i>	<i>x</i>	<i>a</i>	<i>b</i>	<i>c</i>	$\epsilon$	period
<i>B</i>	1	-3	0.845770	506	500		4	2002
<i>A</i>	2	-7	0.846132					
<i>B</i>	11	-29	0.858303	27	268		4	1074
<i>A</i>	-2	3	0.870475					
<i>B</i>	3	-9	0.935237		14		2	58

TABLE III

Same as Table I for side *A - B*

<i>ABC</i>	<i>p</i>	<i>q</i>	<i>x</i>	<i>a</i>	<i>b</i>	<i>c</i>	$\epsilon$	period
<i>B</i>	-1	2	0.272883		2		2	10
<i>A</i>	0	-2	0.545766	3				
<i>B</i>	-5	10	0.630711		10		4	42
<i>A</i>	-4	8	0.715657	14				
<i>B</i>	-5	12	0.727983		46		4	186
<i>A</i>	4	-12	0.740309	75				
<i>B</i>	3	-8	0.746177		309		3	1238
<i>A</i>	6	-16	0.752046	541				
<i>B</i>			0.752047		292429		4?	1169718
<i>A</i>			0.752048	584314				
<i>B</i>			0.752050		633953		4?	2535814
<i>A</i>			0.752051	683589				
<i>B</i>			0.752053		349846		4?	1399386
<i>A</i>	-14	32	0.752054	16100				
<i>B</i>	37	-92	0.752060		174383		4?	697534
<i>A</i>			0.752066	332663				
<i>B</i>			0.752068		277320		4?	1109282
<i>A</i>	-18	42	0.752070	221974				
.	.	.	.		.		.	.
.	.	.	.		.		.	.
.	.	.	.		.		.	.
.	.	.	.		.		.	.
<i>C</i>	16	<i>d</i> - 41	0.752086			131251		
<i>B</i>	-15	34	0.752095		171516		2	686066
<i>C</i>	-16	37	0.752104			211780		
<i>B</i>	9	-22	0.752106		120069		2	480278
<i>C</i>	14	-35	0.752107			28357		
<i>B</i>			0.752113		271882		3?	1087530

TABLE III continued

ABC	p	q	x	a	b	c	ε	period
C			0.752119			515405?		
B			0.752119		379033		2?	1516134
C	-12	27	0.752120			242660		
B			0.752120		153144?		2?	612578?
C	8	-21	0.752120			63627		
B	13	-32	0.752126		72921		2	291686
C	-8	17	0.752133			82214		
B	-11	26	0.752183		42350		3	169402
C	-6	13	0.752233			2484		
B	-19	44	0.755350		1270		2	5082
C	4	-11	0.758466			55		
B	-7	16	0.765532		32		3	130
C	2	-7	0.772599			7		
B	-3	6	0.828334		18		2	74
C	-2	3	0.884069			28		
B	1	-4	0.942034		15		3	62

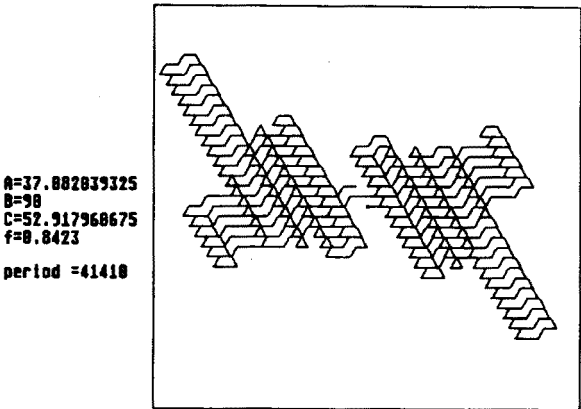


Fig. 11. Velocity portrait of orbit of Fig. 10

3. Bi-orthogonal orbits for arbitrary triangles

For the triangle with  $\alpha_1 = 32.321654$ ,  $\alpha_2 = 82.024024$  and  $\alpha_3 = 65.654322$  the simplest bi-orthogonal orbit has period 12. An example is

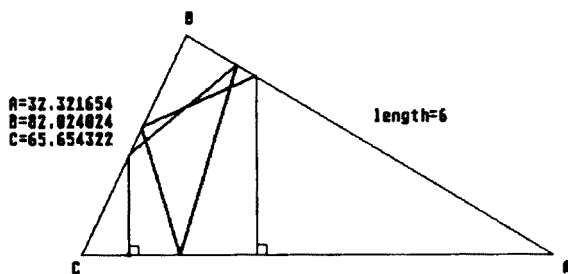


Fig. 12. Bi-orthogonal orbit for triangle with  $A = 32.321654$ ,  $B = 82.024024$ ,  $C = 65.654320$ .

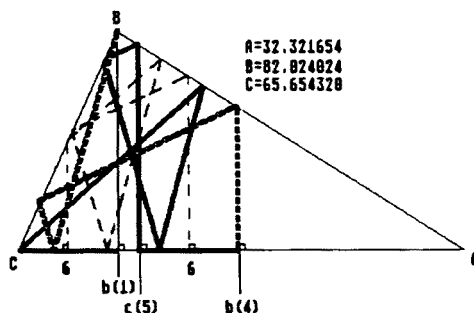


Fig. 13. Construction of limiting orbits

shown in Fig. 12. More details are seen in Fig. 13, where the dashed line consists of 6 steps, which constitute half of the bi-orthogonal orbit.

On the basis line two intervals are marked by heavy lines. Each point of the first interval, when considered as starting point of an orthogonal orbit, is mapped after 6 steps on a point of the second interval, where the orbit hits the base line perpendicularly. The intervals have equal length and the same orientation. The endpoint  $b(1)$  of the first interval is given by a 1-step orthogonal orbit, which starts from  $B$ . The other endpoints  $c(5)$  and  $b(4)$  similarly are given by 5-step and 4-step orthogonal orbits, starting from  $C$  and  $B$  respectively. Once the orthogonal orbits, connecting these endpoints, are found, other bi-orthogonal orbits from one interval to the other can be constructed by drawing path elements parallel to the "endpoint trajectories". This holds not only for the special case shown in Fig. 13, but also in general. The number of steps from one interval to the other can be determined in two ways. Firstly, starting from a point close to the lower limit of the interval on the left,  $L_1$  steps must be taken to come close to the corner from where it takes also  $L_1$  steps to reach this lower limit exactly. In the same way, starting from a point equally close to the lower limit of the interval on the right,  $L_2$  steps must be taken to

come close to the same corner from where it takes also  $L_2$  steps to reach this lower limit exactly. If in addition it takes  $\ell$  steps to turn through this corner to connect the two parts, the total length of the orbit between the two intervals is equal to  $S = L_1 + L_2 + \ell$ . The second way to calculate this  $S$  is by considering two paths which start (equally) close to the upper limits of the left and right interval. If it takes  $R_1$  and  $R_2$  steps to reach a common corner exactly, starting from the upper limits, and if  $r$  is the number of steps for the orbit to turn through this corner in order to connect these two parts, the total length of the orbit between the intervals is now equal to  $S = R_1 + R_2 + r$ . The numbers  $L_1, L_2, R_1, R_2$  can be large, but  $\ell$  and  $r$  are small and limited by the number of times the turn-around-angle is contained in  $\pi$ . This construction also provides a method to find the pairs of intervals which are mapped onto each other by way of bi-orthogonal orbits. Upper and lower limits of the intervals are determined by looking for integers  $q_1, q_2, q_3$ , such that orbits starting from the corners  $A, B$  and  $C$  with angles  $\theta_0 = q_1\alpha_1 + q_2\alpha_2 + q_3\alpha_3 + \pi/2$  will hit a side perpendicular before 50,000 steps are taken. Given these upper and lower limits a point of the interval is taken as starting point of an orthogonal orbit. In this way the length  $S$  of the orbit is determined, as well as the position of the twin interval. The numbers  $\ell = S - L_1 - L_2$  and  $r = S - R_1 - R_2$  turn out always to be small, which is consistent with the picture as sketched above. Table IV contains the results obtained in this way. It shows the position of forty intervals numbered from 1 to 40. In column 7 the pairs of twinned intervals are indicated.

Although only 64.6% of the base line is covered by these forty intervals, it is expected that an infinite number of them exists. In this case there should be (at least) one accumulation point. There is, however, no indication yet where it should be located.

The same analysis can be repeated for obtuse triangles. An example is shown in Fig. 14. If the succession in which the orbit hits the sides is taken for granted, the reader will have no difficulty in convincing himself that the orbit indeed is bi-orthogonal with period 20.

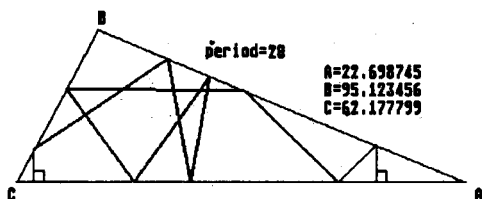


Fig. 14. Bi-orthogonal orbit for obtuse triangle with  $A = 22.698745$ ,  $B = 95.123456$ ,  $C = 62.177799$ .



TABLE IV

Partitioning of side  $C - A$  of acute triangle into pairs of intervals, which are connected by bi-orthogonal orbits. Angles:  $A = 32.321654$ ,  $B = 82.024024$ ,  $C = 65.654320$ , ABC: Corner of departure,  $\theta = 90 + q_1 * A + q_2 * B + q_3 * C$ : angle of departure,  $f$ : point of orthogonal incidence on side  $C - A$ ,  $L/R$ : number of steps until incidence on side  $C - A$ ,  $n - m$ : interval  $n$  mapped onto interval  $m$ ,  $S$ : length of orbit between intervals  $n$  and  $m$ ,  $l/r$ : number of turn around steps in orbit from lower/upper limit of the interval 0.646288: fraction of  $C - A$  covered by 40 intervals.

ABC	$q_1$	$q_2$	$q_3$	$f$	$L/R$	$n - m$	$S$	$l$	$r$
$B$	-1	0	0	0.222566	1	1 - 5	6	1	1
$A$	-3	6	-1	0.238287	14	2 - 37	22	1	4
$C$	-8	10	2	0.245464	52	3 - 36	194	1	1
$B$	1	2	-2	0.252706	173	4 - 32	364	1	4
$A$	8	-13	-2	0.258068	39				
$C$	1	-1	-1	0.270370	5	5 - 1	6	1	1
$B$	-2	-1	1	0.492936	4				
$C$	8	2	-8	0.498745	1566	6 - 27	5094	2	1
$B$	-2	9	-3	0.498913	382				
$C$	-6	-4	6	0.514208	16	7 - 13	132	1	1
$B$	5	4	-6	0.530701	77				
$A$	-3	-4	3	0.531519	152	8 - 21	266	5	4
$A$	-7	14	-1	0.534296	246				
$C$	-2	-2	2	0.563951	6	9 - 31	188	1	2
$C$	0	-2	0	0.571747	2				
$C$	5	1	-5	0.582741	2947	10 - 14	3052	2	2
$C$	11	-1	-9	0.583062	2479	11 - 35	2696	2	1
$B$	7	0	-6	0.583689	2623	12 - 23	4050	1	2
$C$	-8	-6	8	0.584001	3588				
$C$	-5	-5	5	0.586973	115	13 - 7	132	1	1
$B$	4	3	-5	0.603465	54				
$C$	-3	-3	3	0.613199	103	14 - 10	3052	2	2
$C$	-13	1	9	0.613520	571				
$B$	-5	-2	4	0.617811	57	15 - 18	824	1	4
$A$	0	-7	2	0.618843	313				

TABLE IV continued

<i>ABC</i>	$q_1$	$q_2$	$q_3$	$f$	$L/R$	$n - m$	$S$	$l$	$r$
<i>B</i>	-4	-5	5	0.624320	1312	16 - 28	1406	1	1
<i>B</i>	-7	2	4	0.625201	137				
<i>C</i>	-2	-8	4	0.655749	426	17 - 33	962	2	1
<i>B</i>	-4	-1	3	0.659416	766	18 - 15	824	1	4
<i>A</i>	0	3	-2	0.660449	507				
<i>C</i>	4	10	-8	0.701889	338	19 - 29	844	2	2
<i>B</i>	4	-1	-3	0.702772	68				
<i>B</i>	2	-3	-1	0.703024	118	20 - 39	186	1	4
<i>A</i>	-4	1	2	0.708103	109	21 - 8	266	5	4
<i>A</i>	5	-10	-1	0.710880	16	22 - 40	94	5	2
<i>A</i>	-1	2	-1	0.713824	92				
<i>B</i>	8	1	-7	0.725348	1426	23 - 12	4050	1	2
<i>C</i>	10	4	-10	0.725661	460				
<i>C</i>	0	-6	2	0.753609	76	24 - 38	112	1	1
<i>B</i>	0	-5	1	0.771747	44	25 - 34	462	2	4
<i>A</i>	2	-1	-2	0.776983	427	26 - 30	442	5	1
<i>B</i>	-2	-5	3	0.782882	190				
<i>C</i>	-10	-2	8	0.791807	3526	27 - 6	5094	2	1
<i>B</i>	-1	10	-4	0.791975	4711				
<i>B</i>	-5	-6	6	0.809996	93	28 - 16	1406	1	1
<i>B</i>	-8	1	5	0.810876	1268				
<i>C</i>	-6	-10	8	0.849731	504	29 - 19	844	2	2
<i>B</i>	-6	-1	5	0.850614	774				
<i>A</i>	3	-6	-1	0.871435	10	30 - 26	442	5	1
<i>B</i>	-1	-4	2	0.877334	251				
<i>C</i>	-1	-3	1	0.883686	181	31 - 9	188	1	2
<i>C</i>	2	0	-2	0.891483	184				
<i>B</i>	2	3	-3	0.899423	190	32 - 4	364	1	4
<i>A</i>	-8	9	2	0.904785	321				
<i>C</i>	0	8	-4	0.907878	534	33 - 17	962	2	1
<i>B</i>	-3	0	2	0.911546	195				

TABLE IV continued

$ABC$	$q_1$	$q_2$	$q_3$	$f$	$L/R$	$n - m$	$S$	$l$	$r$
$B$	0	5	-3	0.913757	416	34 - 25	462	2	4
$A$	-2	-3	2	0.918993	31				
$C$	-9	-1	7	0.920861	215	35 - 11	2696	2	1
$B$	6	-1	-5	0.921488	72				
$C$	-7	9	1	0.944886	141	36 - 3	194	1	1
$B$	0	1	-1	0.952128	20	37 - 2	22	1	4
$A$	1	-2	-1	0.967848	4				
$C$	1	-7	1	0.973838	35	38 - 24	112	1	1
$B$	1	-4	0	0.991977	67	39 - 20	186	1	4
$A$	4	-5	-2	0.997055	73	40 - 22	94	5	2

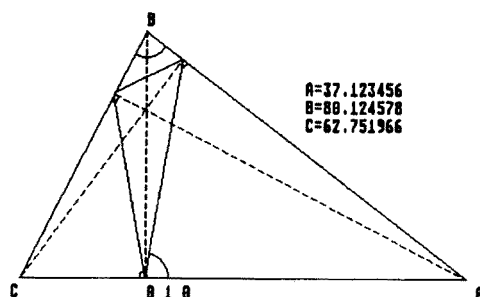


Fig. 15. Period-3 orbit in acute triangle with  $A = 37.123456$ ,  $B = 80.124578$ ,  $C = 62.751966$ .

#### 4. Integer periodic orbits

In the previous two Sections it was shown that each side of a triangle can be divided into pairs of intervals which are mapped onto each other by way of bi-orthogonal orbits. For orthogonal triangles the two intervals of each pair are touching each other, while for arbitrary triangles there is a gap in between. In this Section integer periodic orbits — with  $\theta = q_1\alpha_1 + q_2\alpha_2 + q_3\alpha_3$  — will be considered and the question will again be asked whether it is possible to dissect each side into sets of intervals which are mapped onto intervals of the same set by orbits all with the same starting angle, but not necessarily with the same period.



Fig. 15 shows the standard construction of a period-3 orbit in an acute triangle. The starting angle is given by  $(q_1, q_2, q_3) = (0, 1, 0)$ . In Fig. 16 it is seen how this period doubles when the base point is shifted. The largest possible shift (figure 17) is obtained when two collision points coalesce in a corner of the triangle. The same sequence occurs in Figs 18-20 for a period-5 orbit. It should be noted — by the way — that the period-5 orbit of Fig. 18 can be seen as a period-3 orbit in the larger triangle  $ABC'$  obtained by reflecting  $B$  in side  $AC$ , calling it  $B'$  and constructing  $C'$  as the intersection of  $AB'$  with  $BC$ . In Fig. 17 some intervals on the sides are heavily shaded. Each of these intervals is mapped onto itself after half of the period-6 integer orbit has been traversed. The orientation is thereby reversed. The same phenomenon is seen in Fig. 20, where a number of intervals are specially marked. Each is mapped onto itself by the same period-10 integer orbit, traversed in one direction. For each interval other starting angles can be found by reversing this direction, i.e., by changing  $(q_1, q_2, q_3)$  into  $(1 - q_1, 1 - q_2, 1 - q_3)$ .

Figs 17 and 20 suggest a method for finding intervals which are mapped onto themselves by integer periodic orbits: for a point infinitesimally close to a corner (and on either side) try to find directions  $\theta = q_1\alpha_1 + q_2\alpha_2 + q_3\alpha_3$ , such that an orbit starting into this direction will be periodic. Once such a direction is found the starting point is shifted away from the corner, thereby maintaining the direction, until the orbit changes its period. In this way a number of periodic intervals with a corner at one of the boundaries were found. They are listed in Table V. Each of these intervals is of course mapped by the orbit on many subintervals of the sides, but only for a limited number of them the collision angle will be the same as for the original interval. Consider, for example, an orbit with period 274, which starts from the side  $C - A$  at a distance from  $C$  between 0.95861 and 1.0 (i.e., close to  $A$ ) and with an angle of 14.133564 degrees. There are four different points on the orbit where it hits the side  $C - A$  with the same angle. First after 64 steps, then after 73 steps, then again after 64 steps and finally again after 73 steps to complete the periodic orbit. The process is shown in Fig. 21. The four intervals have equal lengths and two intervals which are connected by an odd number of steps have opposite orientation. The analogous decomposition of the period -2094 orbits is given in Fig. 22. All paths, except the ones marked with 372 and 603, have a length of 12 steps. The intervals with this period and with a starting angle given by  $(q_1, q_2, q_3) = (-6, 0, 4)$ , cover a fraction of 9.5% of the side  $B - C$ . In Fig. 21 this fraction is 16.6% of side  $C - A$  for the intervals with a period of 274 and an angle given by  $(q_1, q_2, q_3) = (-3, 0, 2)$ . This fraction increased to 20.5% after it was discovered that there are two more intervals on  $C - A$  with the same starting angle, but with periods of 90 and 150, both listed in Table V.

TABLE V

Intervals with integer periodic orbits  $A = 37.123456$ ,  $B = 80.124578$ ,  
 $C = 62.751966$ ,  $\theta = q_1 * A + q_2 * B + q_3 * C$

side	interval	$q_1$	$q_2$	$q_3$	$\theta$	period	covered
$A - B$	0.88357 - 1.00000	0	0	1	62.751966	$6 = 3 + 3$	0.233
$B - C$	0.00000 - 0.25264	1	0	0	37.123456	$6 = 3 + 3$	0.505
$A - B$	0.61838 - 1.00000	-1	0	1	25.628510	$10 = 5 + 5$	0.763
$B - C$	0.00000 - 0.25264	2	0	0	74.246912	$10 = 5 + 5$	0.505
$C - A$	0.00000 - 0.08298	-2	1	0	5.877666	$30 = 15 + 15$	0.166
$C - A$	0.00000 - 0.01133	3	0	-1	48.618402	$30 = 15 + 15$	0.023
$C - A$	0.00000 - 0.02516	-3	1	1	31.506176	$58 = 29 + 29$	0.050
$C - A$	0.00000 - 0.03367	4	0	-2	22.989892	$58 = 29 + 29$	0.067
$C - A$	0.00000 - 0.00615	-2	-1	3	33.884408	$90 = 45 + 45$	0.012
$C - A$	0.00000 - 0.00973	3	2	-4	20.611660	$90 = 45 + 45$	0.019
$C - A$	0.26667 - 0.28070	-3	0	2	14.133564	$90 = 45 + 45$	0.028
$C - A$	0.13339 - 0.13910	-3	0	2	14.133564	$150 = 75 + 75$	0.012
$B - C$	0.00000 - 0.00428	5	2	-5	32.106606	$150 = 6 + 69$ + $6 + 69$	0.017
$C - A$	0.96615 - 1.00000	0	1	-1	17.372613	$274 = 73 + 64$ + $73 + 64$	0.135
$C - A$	0.95861 - 1.00000	-3	0	2	14.133564	$274 = 64 + 73$ + $64 + 73$	0.166
$C - A$	0.99454 - 1.00000	0	-2	3	28.006742	$278 = 109 + 30$ + $109 + 30$	0.022
$B - C$	0.00000 - 0.00592	-6	0	4	28.267128	$2094 = 372 + 12$ + $12 + 12$ + $603 + 12$ + $12 + 12$ + $372 + 12$ + $12 + 12$ + $603 + 12$ + $12 + 12$	0.095

No systematic effort was made to find more periodic intervals on  $C - A$  with the same  $(q_1, q_2, q_3)$ , because it turned out that, if they exist at all, their period is 10,000 or higher. The evidence for the corrections of the second conjecture, therefore, is not very convincing. However, it is not yet disproved either.

At this point it may not be irrelevant to mention that, although in a

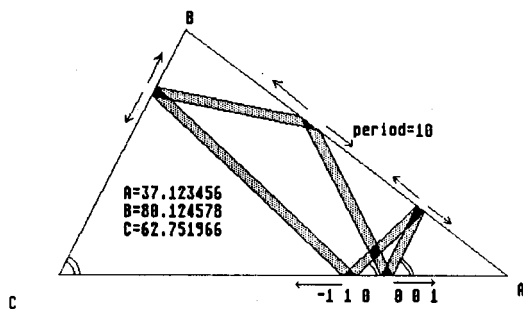


Fig. 19. Doubling of the period-5 orbit

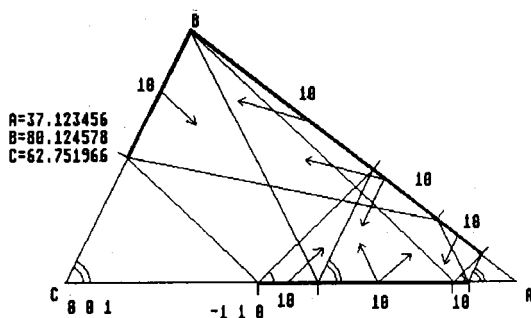


Fig. 20. Limits for the period-10 orbits

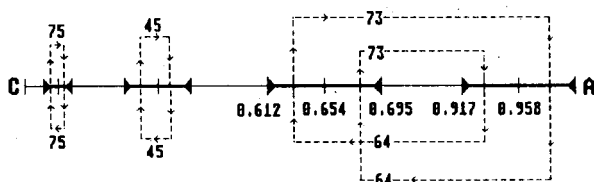


Fig. 21. Mapping of intervals of  $C - A$  onto themselves. Return to  $C - A$  with the same angle of  $14.133564$  degrees after indicated number of steps.

two-dimensional random walk the probability eventually to reach the origin is one hundred percent, the expected pathlength is infinite [11].

## 5. Miscellaneous

So far only acute triangles were studied extensively. Only one example of a bi-orthogonal orbit in an obtuse triangle was given in Fig. 14 while another one is shown in Fig. 23. It is, however, not difficult to perform a

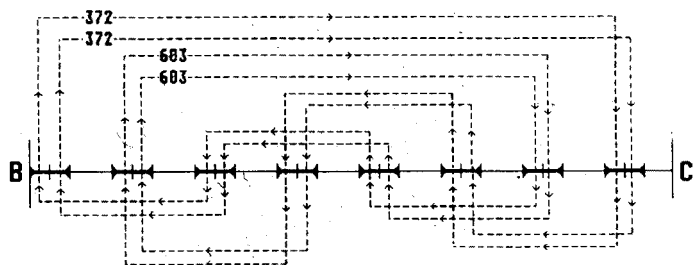


Fig. 22. Same as in Fig. 21 for side  $B - C$  with return angle  $= -6A + 4C = 28.267128$  degrees.

more extended analysis like for acute triangles. The evidence assembled so far further supports the correctness of the first conjecture that all mono-orthogonal orbits are indeed bi-orthogonal.

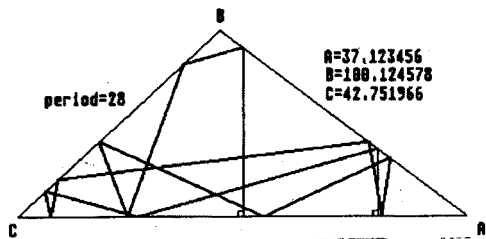


Fig. 23. Bi-orthogonal orbit for obtuse triangle with  $A = 37.123456$ ,  $B = 100.124578$  and  $C = 42.751966$  degrees.

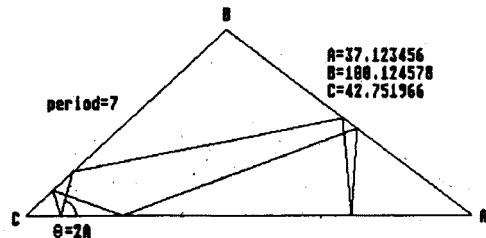


Fig. 24. Integer period-7 orbit in obtuse triangle with  $A = 37.123456$ ,  $B = 100.124578$ ,  $C = 42.751966$ .



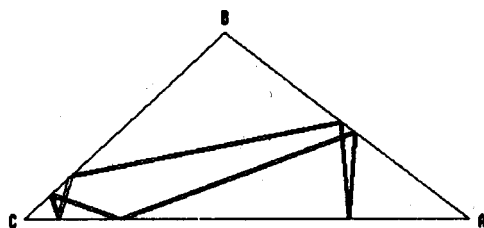


Fig. 25. Doubling of the period-7 orbit

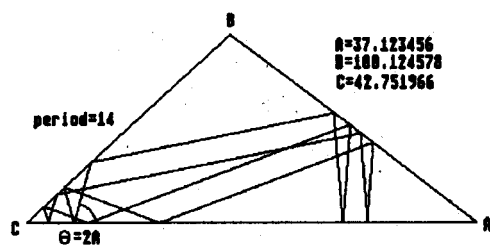


Fig. 26. Another period-14 integer orbit

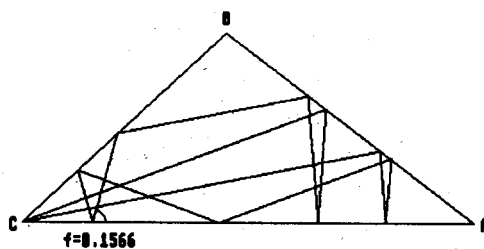


Fig. 27. Limits for the period-14 integer orbits

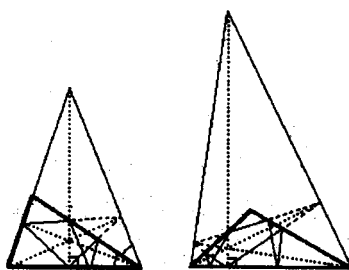


Fig. 28. How to construct period-5 and period-7 orbits

The second conjecture requires the construction of integer periodic orbits. For obtuse triangles this has not been done on a large scale yet, but the series of pictures 24-27 shows that in principle it is feasible. Starting from a period-7 integer orbit (Fig. 24), period doubling occurs (Figs 25 and 26), until the orbit hits a corner (Fig. 27). Actually, in a systematic approach, first two integer directions emanating from a corner must be found, such that they match to form a periodic orbit. The collision points with the sides then fix the intervals with the same period. Again many examples of integer periodic intervals in obtuse triangles have been found in this way. They support the second conjecture, but an almost full covering of the sides by these periodic intervals has not been achieved yet. A general method for constructing integer orbits of periods 5 and 7, starting from a period-3 integer orbit, is shown in Fig. 28.

The third conjecture about the non-existence of periodic weak-orthogonal orbits is confirmed so far, because after an extensive search none has been found yet. The same can be said about periodic orbits with arbitrary starting angles, so that it is not too outrageous to claim the

*4th Conjecture:* In an irrational triangle all periodic orbits are of the integer- or of the half-integer type.

The reader who has reached this point probably does not need further justification for doing this kind of work. For those, however, who started reading at the end, it may be interesting to note that the study of classical periodic orbits can be very helpful in classifying and even calculating molecular spectra. A review paper on this subject was recently written by J. Zakrzewski [12]. Therefore it is not excluded that by measuring the spectrum of cavities with a triangular cross section the periodic orbits constructed in this paper will be of some help in explaining the data.

The author is grateful for the special way in which Dr. J. Groeneveld has contributed to this paper.

## REFERENCES

- [1] A. Hobson, *J. Math. Phys.* **16**, 2210 (1975).
- [2] G. Casati, J. Ford, *J. Comp. Phys.* **20**, 97 (1976).
- [3] Y.G. Sinai, *Introduction to Ergodic Theory*, Princeton U.P., Princeton, 1976.
- [4] F. Rabouw, Th.W. Ruijgrok, *Physica* **109A**, 500 (1981).
- [5] G.A. Galperin, *Commun. Math. Phys.* **91**, 187 (1983).
- [6] E. Gutkin, *Physica* **19D**, 311 (1986).
- [7] A.N. Zemlyakov, A.B. Katok, *Math. Notes* **18**, 760 (1975); erratum: **20**, 1050 (1976).
- [8] C. Boldrighini, M. Keane, F. Marchetti, *The Annals of Probability* **6**, 532 (1978).

- [9] A. Katok, *Israel J. of Math.* **35**, 301 (1980).
- [10] H. Masur, *Duke Math. Journal* **53**, 307 (1986).
- [11] See e.g. J.W. Sanders, Th.W. Ruijgrok, J.J. ten Bosch, *Journ. Math. Phys.* **12**, 534 (1971).
- [12] J. Zakrzewski, *Acta Phys. Pol.* **A77**, 745 (1990). See also, M.C. Gutzwiller, *Chaos in Classical and Quantum Mechanics*, Springer, Berlin 1991.